Journal of Natural Gas Science and Engineering 15 (2013) 38–52

Contents lists available at ScienceDirect

Journal of Natural Gas Science and Engineering

journal homepage: www.elsevier.com/locate/jngse

Roles of coal heterogeneity on evolution of coal permeability under unconstrained boundary conditions

Zhongwei Chen [a, *], Jishan Liu [b], Derek Elsworth [c], Zhejun Pan [d], Shugang Wang [c]

[a] School of Mechanical and Mining Engineering, The University of Queensland, Brisbane, QLD 4072, Australia
[b] School of Mechanical and Chemical Engineering, The University of Western Australia, WA 6009, Australia
[c] Department of Energy and Mineral Engineering, Penn State University, PA 16802-5000, USA
[d] CSIRO Earth Science and Resource Engineering, Private Bag 10, Clayton South, Victoria 3169, Australia

ARTICLE INFO

Article history:
Received 5 January 2013
Received in revised form
6 August 2013
Accepted 12 September 2013
Available online 2 October 2013

Keywords:
Coal permeability
Gas sorption
Coal swelling
Coal–gas interaction
Local heterogeneity

ABSTRACT

Coal permeability models based on constrained conditions such as constant volume theory can successfully match unconstrained experimental data and field observations. However, these models have a boundary mismatch because the boundary of permeability models is constrained while experiment boundary is free displacement or unconstrained. What the mechanism is to require such a boundary mismatch has not been well understood. In this study, a full coupled approach was developed to explicitly simulate the interactions of coal matrixes and fractures. In this model, a matrix-fracture model is numerically investigated after incorporating heterogeneous distributions of Young's modulus, Langmuir strain constant in the vicinity of the fracture. The impact of these local heterogeneities of coal mechanical and swelling properties on the permeability evolution is explored. The transient permeability evolution during gas swelling process is investigated and the difference between the final equilibrium permeability and transient permeability is compared. With the heterogeneity assumption, a net reduction of coal permeability is achieved from the initial no-swelling state to the final equilibrium state. This net reduction of coal permeability increases with the fracture (injection) pressure and is in good agreement with laboratorial data under the unconstrained swelling conditions. Coal local heterogeneity in vicinity of fracture can therefore be the mechanism of the above mismatch.

1. Introduction

The permeability of coal is a key attribute in determining coalbed methane production and CO_2 storage in coal seam reservoirs. Coal permeability is often determined by regular sets of fractures called cleats, with the aperture of the cleats being a key property in the magnitude of the permeability (Connell et al., 2010). The relative roles of stress level, gas pressure and composition, fracture geometry of coal and water content are intimately connected to the processes of gas sorption, transport and coal swelling/shrinkage (Liu et al., 2011a).

Significant experimental efforts have been made to investigate coal permeability and its evolution. Laboratory measured permeabilities of coal to adsorbing gasses, such as CH_4 and CO_2, are known to be lower than permeabilities to non-absorbing or lightly adsorbing gasses such as argon and nitrogen (Durucan and Edwards, 1986; Siriwardane et al., 2009; Somerton et al., 1975). Under constant total stress, permeability to adsorbing gas decreases with increasing pore pressure due to coal swelling (Chen et al., 2011; Mazumder and Wolf, 2008; Pan et al., 2010a; Robertson, 2005; Wang et al., 2010, 2011), and increases with decreasing pore pressure due to matrix shrinkage (Cui and Bustin, 2005; Harpalani and Schraufnagel, 1990; Harpalani and Chen, 1997; Seidle and Huitt, 1995). It is also impacted by the presence of water and the magnitude of water saturation (Han et al., 2010; Pan et al., 2010b). One thing in common for the above studies is that they were conducted under unconstrained boundary conditions.

A number of proposed coal permeability models have been developed to match experimental data (Cui and Bustin, 2005; Izadi et al., 2011; Liu and Rutqvist, 2010; Palmer and Mansoori, 1998; Pekot and Reeves, 2002; Seidle and Huitt, 1995; Shi and Durucan, 2004; Wang et al., 2011; Zhang et al., 2008). Two assumptions are applied to these models – uniaxial strain and constant overburden or confining stress (Connell et al., 2010; Liu et al., 2011a). These models have been mostly successful in matching experimental data that were conducted under stress-controlled (unconstrained)

* Corresponding author. Tel.: +61 07 3365 3472.
E-mail address: zhongwei.chen@uq.edu.au (Z. Chen).

1875-5100/$ – see front matter © 2013 Elsevier B.V. All rights reserved.
http://dx.doi.org/10.1016/j.jngse.2013.09.002

boundary conditions. However, permeability models derived under stress-controlled condition assumption are incapable of matching experimental data, particularly for the models developed with the matchstick or cubic coal geometry. This is because matrix swelling does not affect coal permeability due to the complete separation between matrix blocks caused by through-going fracture. In this case, for a given fracture pore pressure, the swelling results in an increase of fracture spacing, rather than a change in fracture aperture (Liu and Rutqvist, 2010). However, this has not been consistent with laboratory observations that show significant coal permeability variation due to matrix swelling under constant confining stress conditions (Chen et al., 2011; Lin et al., 2008; Pan et al., 2010a). This behaviour remains enigmatic as the permeability of the porous coal is determined by the effective stress only.

A few studies were carried out on either improving current permeability models or explaining why permeability models developed under uniaxal strain condition are capable of matching experimental data. Connell et al. (2010) partitioned the sorption strain into bulk, pore and matrix strains in contrast to existing approaches, and derived several different forms of the permeability models for the distinct geometric and mechanical arrangements that can be encountered with laboratory testing. Liu and Rutqvist (2010) believed that in reality coal matrix blocks are not completely separated from each other by fractures but connected by the coal-matrix bridges, and developed a new coal-permeability model for constant confining-stress conditions, which explicitly considers fracture–matrix interaction during coal-deformation processes based on the internal swelling stress concept. An alternative reasoning has been investigated by J. Liu et al. (2010a), considering the internal actions between coal fractures and matrix. Recently, Izadi et al. (2011) proposed a mechanistic representation of coal as a collection of unconnected cracks in an elastic swelling medium, where voids within a linear solid are surrounded by a damage zone. In the damage zone the Langmuir swelling coefficient decreases outwards from the wall and the modulus increases outwards from the wall. In the analysis, fluid pressures are applied uniformly throughout the body, so it is incapable of observing the transient permeability evolution due to coal–gas interactions during gas transport. J. Liu et al. (2011b) addressed the same phenomena from different point of view, stating that coal permeability is controlled by the switching process between local swelling and macro-swelling, and the extent of switching of coal swelling determines coal permeability is higher or lower than initial value.

However, these studies still have three limitations that need to be improved: (1) they were generally carried out on the assumption of homogeneity, where coal properties were assumed to be same throughout the whole domain; (2) permeability value is assumed to be only related to pore pressure and effective stress, so with the same pore pressure the permeability value is same; and (3) permeability is independent of time. These assumptions have been conflict with many experimental observations. For instance, Maggs (1946) investigated the feature of coal swelling, and shown that in the presence of an adsorbed film, coal swells and a weakening of the structure would result on adsorption. This phenomenon was also observed by Hsieh and Duda (1987). The effect of high-pressure CO_2 on the macromolecular structure of coal has been studied by Mirzaeian and Hall (2006), and showed that the glass transition temperature of coal decreases with CO_2 pressure significantly, indicating that high-pressure CO_2 diffuses through the coal matrix causes significant plasticization effects, and changes the macromolecular structure of coal. Similar observation was obtained by many other researchers (Larsen, 2004; Goodman et al., 2005; John, 2004; C.J. Liu et al., 2010; White et al., 2005). The thermodynamics and mechanism for this phenomenon was examined by Mirzaeian and Hall (2008). The plasticization effects of coal adsorption have been verified by the weakening of coal mechanical strength from experimental measurements (Ates and Barron, 1988; Ranjith et al., 2010; Viete and Ranjith, 2006, 2007; Wang et al., 2011). Recently, Siriwardane et al. (2009) found that permeability of adsorbing gas in coal is a function of gas exposure time.

The non-homogeneous feature of coal swelling has also been observed by other approaches (Day et al., 2008; Karacan and Okandan, 2001; Karacan, 2003, 2007) as apparent from quantitative X-ray CT imaging and from optical methods. Gibbins et al. (1999) examined the heterogeneity of coal samples by means of density separation and optical and scanning electron microscopy, and found that a high degree of heterogeneity exists between average compositions for the different density cuts within each sample, between different particles within the same density cuts and within the particles themselves. Similar work was conducted by Gathitu et al. (2009). Manovic et al. (2009) presents the microscopic observations of coals of different ranks and mineral matter contents, showing an increasing of heterogeneity with mineral matter content. Anisotropic swelling induced by chemical heterogeneity of coal was also seen (Douglas, 1984; French et al., 1993; Pone et al., 2010).

As summarized above, the real behaviours of the sorption-induced swelling/shrinkage of coal are far different from the homogeneous assumption that is generally made for theoretical permeability analysis. The effects of coal chemical heterogeneity and swelling are mutual. The heterogeneity of coal brings the non-homogeneous distribution of coal swelling strain, and meanwhile coal swelling causes the heterogeneous distribution coal physical property (e.g. Young's modulus). In this study, it is considered that the heterogeneities of coal physical properties and swelling strain are responsible for the enigmatic behaviour of coal permeability reduction with adsorbing gas injection under unconstrained conditions. To prove this, a fully coupling numerical model is conducted to simulate the dynamic interactions between coal matrix swelling and fracture aperture alteration, and translate these interactions to transient permeability evolution. In this numerical model, swelling coefficient and Young's modulus are assumed to vary spatially, and numerical predictions are then compared with observed magnitudes of permeability change in coal. This work is trying to explain why permeability changes with absorbing gas injection even under stress controlled conditions.

2. Theoretical evaluation of coal permeability models

2.1. General coal permeability model

It is clear that there is a relationship between porosity, permeability and the grain-size distribution in porous media. Chilingar (1964) defined this relationship as

$$k = \frac{d_e^2 \phi^3}{72(1-\phi)^2} \tag{1}$$

where k is the permeability, ϕ is porosity and d_e is the effective diameter of grains. Based on this equation, we obtain

$$\frac{k}{k_0} = \left(\frac{\phi}{\phi_0}\right)^3 \left(\frac{1-\phi_0}{1-\phi}\right)^2 \tag{2}$$

When the porosity is much smaller than 1 (normally less than 10%), the second term of the right-hand side asymptotes to unity. This yields the cubic relationship between permeability and porosity for coal matrix

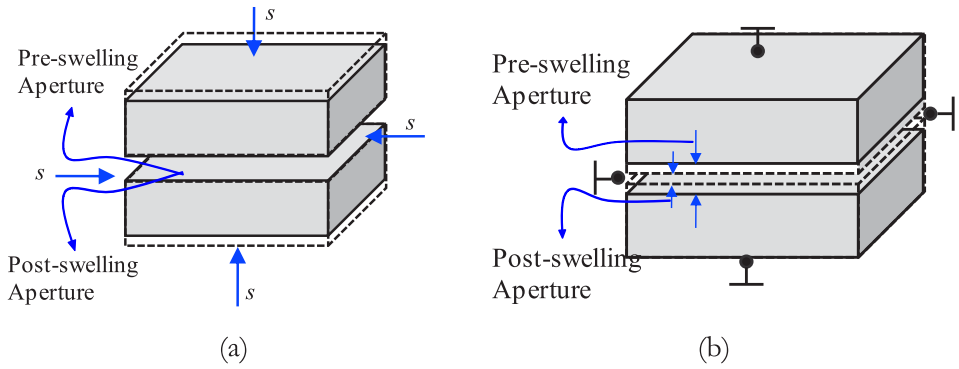

Fig. 1. Schematic diagram of two extreme cases: (a) unconstrained case (free swelling model), where constant stress conditions are applied throughout the whole process; (b) constrained case (constant volume model), where constant volume conditions are maintained throughout the whole process. These two cases represent the lower and upper bounds for permeability and porosity response.

$$\frac{k}{k_0} = \left(\frac{\phi}{\phi_0}\right)^3 \tag{3}$$

Coal porosity can be defined as a function of the effective strain (J. Liu et al., 2010a; 2010b)

$$\frac{\phi}{\phi_0} = 1 + \frac{\alpha}{\phi_0}\Delta\varepsilon_e \tag{4}$$

Substituting Equations (4) into (3) gives

$$\frac{k}{k_0} = \left[1 + \frac{\alpha}{\phi_0}\Delta\varepsilon_e\right]^3 \tag{5}$$

where

$$\Delta\varepsilon_e = \Delta\varepsilon_v + \frac{\Delta p}{K_s} - \Delta\varepsilon_s \tag{6}$$

or

$$\Delta\varepsilon_e = -\frac{\Delta\sigma - \Delta p}{K} \tag{7}$$

where $\Delta\varepsilon_e$ is defined as the incremental of total effective volumetric strain, which is the strain responsible for permeability change, $\Delta\varepsilon_v$ is the total volumetric strain incremental, defined as$\Delta\varepsilon_{11} + \Delta\varepsilon_{22} + \Delta\varepsilon_{33}$, $\Delta p/K_s$ is coal compressive strain incremental, $\Delta\varepsilon_s$ is the incremental of gas sorption-induced volumetric strain, and K_s represents the bulk modulus of coal grains.

Equations (4) and (5) are for coal porosity and permeability which are derived based on the fundamental principles of poroelasticity. They can be applied to the evolution of coal porosity and permeability under variable boundary conditions.

Coal porosity and permeability can be defined as a function of either effective strain (Eq. (6)) or effective stress (Eq. (7)). However, coal porosity and permeability models may have a variety of forms when specific conditions are imposed. Examples include:

- When the change in total stress is equal to zero, i.e. $\Delta\sigma = 0$, both coal porosity and permeability are independent of the total stress. Under this condition, they can be defined as a function of gas pressure only.
- Assuming coal sample is under conditions of uniaxial strain and the overburden load remains unchanged, they can also be defined as a function of gas pressure only. However, as the total volumetric strain is different from the zero total stress case, the effective volumetric strain value will be different as well, as illustrated in Eq. (6).
- When the impact of coal fractures and gas compositions is considered, coal porosity and permeability models can be linked to fracture parameters and gas concentrations.

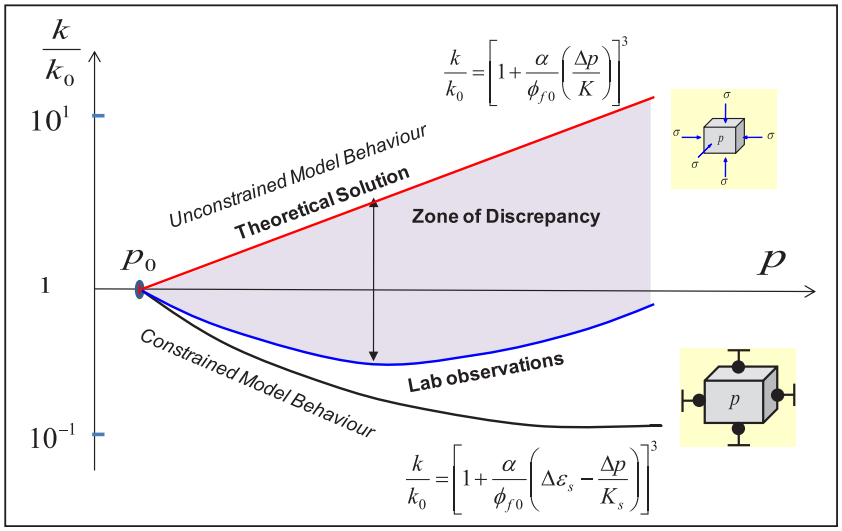

Fig. 2. Illustration of discrepancy for unconstrained swelling case (Liu et al., 2011a).

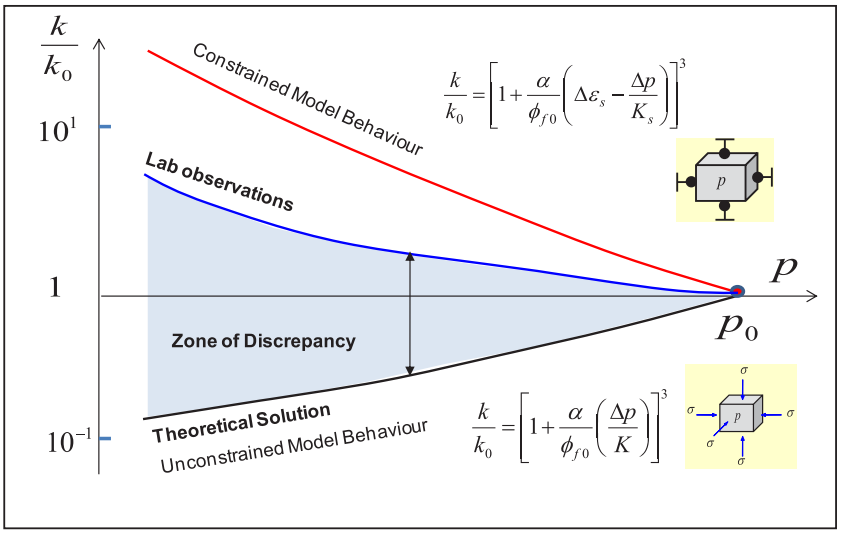

Fig. 3. Illustration of discrepancy for unconstrained shrinkage case (Liu et al., 2011a).

2.2. Permeability evaluation for two boundary conditions

In this section, general coal permeability models are evaluated through comparing laboratorial and in-situ measurements with theoretical solutions of the two extreme cases: the unconstrained shrinkage/swelling case and the constrained case, as illustrated in Fig. 1.

We assume that matrix blocks are completely separated from each other in a coal sample. For the unconstrained model, matrix swelling does not affect coal fracture permeability, because for a given pore pressure coal matrix swelling results in swelling of the blocks alone, rather than changes in fracture aperture. The ambient effective stress also exerts no influence on matrix swelling, due to the complete separation between matrix blocks caused by through-going fractures. However, when coal sample is completely constrained from all directions, coal matrix swelling will be completely transferred to the reduction in fracture apertures. For the constrained model, the entire swelling/shrinkage strain contributes to coal permeability change provided the fractures are much more compliant than coal matrix.

Equation (5) is derived based on the poroelastic theory without the effect of fractures. Therefore, the porosity should be the matrix porosity. However, when these models are applied, the fracture porosity is actually used. Evolutions of coal permeability for both unconstrained and constrained conditions can be defined as Equations (8) and (9), respectively.

$$\frac{k}{k_0} = \left[1 + \frac{\alpha}{\phi_{f_0}}\left(\frac{\Delta p}{K}\right)\right]^3 \tag{8}$$

$$\frac{k}{k_0} = \left[1 + \frac{\alpha}{\phi_{f_0}}\left(\Delta\varepsilon_s - \frac{\Delta p}{K_s}\right)\right]^3 \tag{9}$$

Solutions of these two cases and their comparisons with typical observations are illustrated in Figs. 2–4. Many experimental studies

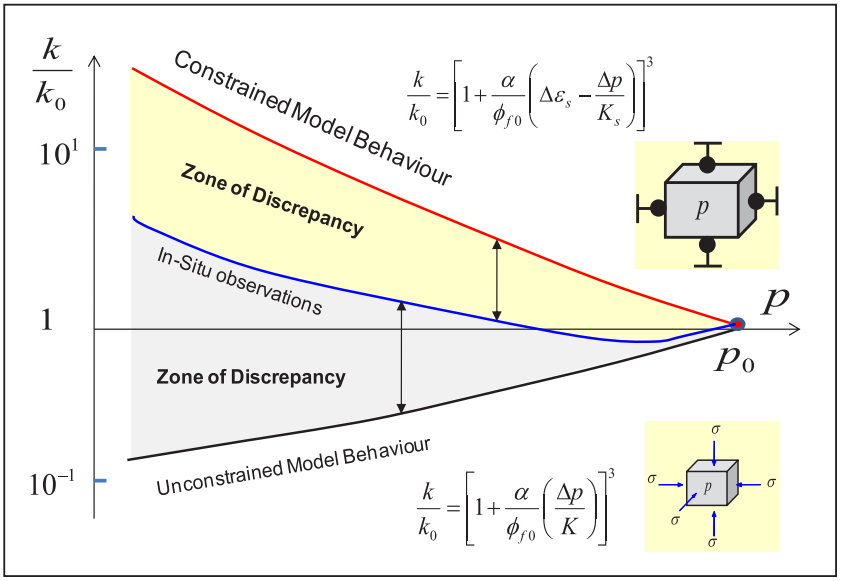

Fig. 4. Illustration of discrepancy between model predicted coal permeability and typical in-situ observations (Liu et al., 2011a).

have been conducted to measure the impact of coal swelling on permeability change with the adsorption of different gasses (Kiyama et al., 2011; Pini et al., 2009; Robertson, 2005; Siriwardane et al., 2009; Wang et al., 2010), observing that even under unconstrained stress-controlled conditions the injection of adsorbing gasses reduces coal permeability at a lower gas pressure and coal permeability may rebound at a higher gas pressure. This observed switch in behaviour is presumably due to the dependence of coal swelling on the gas pressure: coal swelling diminishes at high pressures. Because all of the mentioned experimental observations were made under controlled stress conditions, they should be equal to or close to the theoretical solution under the unconstrained swelling condition. However, the fact points to the contrary, as illustrated in Fig. 2. These observations indicate that although the experiments were conducted under controlled stress conditions the experimental results are more closely related to those monitored under constant volume conditions. These discrepancies indicate the obvious drawbacks of current coal permeability models. If a coal seam gas reservoir is treated as a whole, with full lateral restraint and invariant overburden stress, its behaviour should represent components of the free swelling/shrinkage and the constant volume models. This could explain why current coal permeability models representing conditions of uniaxial strain condition can successfully match some field data.

The influence of coal matrix shrinkage on coal permeability has also been widely studied and an increase with decreasing pore pressure due to matrix shrinkage was observed (Cui and Bustin, 2005; Harpalani and Schraufnagel, 1990; Harpalani and Chen, 1997; Seidle and Huitt, 1995), as shown in Fig. 3. Similar trend has been obtained from field observations, showing that the absolute permeability of coal gas reservoirs increases significantly with continued gas drainage (Cherian et al., 2010; Clarkson et al., 2008, 2010; Sparks et al., 1995; Young et al., 1991). Comparison of field observations with both the unconstrained and constrained models is presented in Fig. 4. Because all of the in-situ observations were made under unknown conditions of the in-situ stress they should lie within the bracketing behaviours. Both Figs. 3 and 4 demonstrate that coal gas reservoirs behave more closely to the constrained (constant volume) case.

The analysis above showed that current coal theoretical permeability models have so far been unsuccessful to explain the results from stress-controlled shrinkage/swelling laboratorial tests, and only some limited success has been achieved in explaining and matching in situ data. The most recent viewpoints (Izadi et al., 2011; Liu and Rutqvist, 2010) have demonstrated that the main reason for the failure is that the impact of coal matrix–fracture compartment interactions on the evolution of coal permeability has not been incorporated appropriately as most of the coal permeability models are derived based on the theory of poroelasticity.

In this work, coal permeability at the state of achieving a uniform matrix swelling/shrinkage is defined as the final equilibrium permeability, but this condition may never be achieved for real coal samples. A difference of the final equilibrium (or ultimate) permeability between an ideal homogeneous coal and a real heterogeneous coal is expected. In the following sections, a simulation model is constructed to investigate the transient permeability evolution during gas swelling process and to study the difference between the final equilibrium permeability and transient permeability, from which the possible mechanism for permeability reduction under unconstrained conditions is discovered. Based on this approach, the important non-linear responses of coal matrix to the effective stress are quantified through the incorporation of heterogeneous distributions of coal properties into complex mechanical coupling with gas transport, where swelling coefficient and modulus vary spatially relative to the fracture void.

3. A heterogeneous matrix–fracture interaction model

Over the past few years, a series of advanced modelling tools has been developed to quantify the complex coal–gas interactions (Chen et al., 2009, 2010; Connell, 2009; Connell and Detournay, 2009; Gu and Chalaturnyk, 2005, 2006; J. Liu et al., 2010a,b, 2011b; Zhang et al., 2008). The key to model the dynamic interactions between coal matrix swelling/shrinkage and fracture aperture alteration is to recover important non-linear responses of coal matrix to the effective stress. A Fully coupled approach has to be chosen to achieve this goal, from which a single set of equations (generally a large system of non-linear coupled partial differential equations) incorporating all of the relevant physics are solved simultaneously. In the following section we applied this fully coupled approach to reproduce the typical enigmatic behaviours of coal permeability evolution with gas injection under unconstrained conditions.

3.1. Numerical model implementation

In the numerical model, the interactions of the fractured coal mass is considered by assuming that cleats do not create a full separation between adjacent matrix blocks but solid rock bridges are present, as illustrated in Fig. 5(a). This assumption is also adapted by other studies (Liu and Rutqvist, 2010; Izadi et al., 2011). We accommodate the role of swelling strains both over contact bridges that hold cleat faces apart and over the non-contacting span between these bridges (Walsh and Grosenbaugh, 1979;

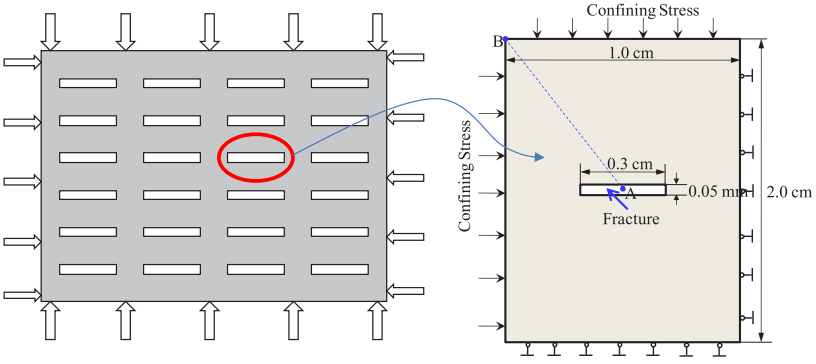

(a) Multiple fracture compartment model (b) Single fracture compartment model

Fig. 5. Numerical model for permeability change under the unconstrained boundary condition. (a) Multiple fracture compartment model (b) Single fracture compartment model.

Table 1
Parameters used in the numerical model.

Parameter	Value
Matrix porosity, %	5.0
Matrix permeability, m^2	5.0×10^{-22}
Viscosity, Pa*s	1.228×10^{-5}
Matrix Young's modulus, GPa	3.45
Poisson's ratio	0.4
Maximum volumetric gas swelling strain	0.03
Gas Langmuir sorption constant, m^3/kg	0.0132
Gas Langmuir pressure constant, MPa	3.96
Coal density, kg/m^3	1500
Young's modulus softening coefficient, α	0.75
Swelling strain reduction factor, β	0.25

Table 2
List of simulation scenarios for homogeneous case.

Simulation scenario	Fracture pressure p_f (MPa)	Young's modulus $\times E_0$	Langmuir strain constant ε_L (%)	Poisson's ratio μ(−)
Case 1	2.0, 4.0, 6.0, 8.0, 10	1.0	3.0	0.40
Case 2	10.0	0.5, 0.75, 1.0, 1.25	3.0	0.40
Case 3	10.0	1.0	1.0, 2.0, 3.0, 4.0	0.40
Case 4	10.0	1.0	3.0	0.25, 0.30, 0.35, 0.40

Yasuhara and Elsworth, 2008). The effects of swelling act competitively over these two components: increasing cleat aperture and permeability due to swelling of the bridging contacts but reducing cleat aperture and permeability due to the swelling of the intervening free-faces. The model exams the influence of effective stress and swelling response for a rectangular crack, just like the matchstick model geometry, and a single component part removed from the array is considered. This represents the symmetry of the displacement boundary condition mid-way between flaws as shown in Fig. 5(b). The change in aperture opening due to the combined influence of coal sorption-induced swelling and effective stress change is simulated during gas transport process, from which the transient permeability evolution is obtained. The cubic relationship between permeability and fracture aperture change was chosen to calculate permeability ratio evolution.

The finite-element numerical tool Comsol Multiphysics 3.5 was used to address this issue. The model considers the following coupled processes: geomechanical deformation of coal matrix, gas flow in coal matrix, and coal matrix adsorption. The model development and implementation details can be found in our other published work (e.g. C.J. Liu et al. (2010)), so there is no need to explain again in this study. The simulation model geometry is 1.0 cm by 2.0 cm with a fracture located at the centre of the model. The length and opening of the fracture are 0.3 cm and 0.05 mm, respectively. Please be noted that the model dimension here refers to the state when the model reaches equilibrium state after applying the confining stress. For coal deformation model, the right and bottom sides are constrained in the normal direction to honour symmetry and the other two sides are stress controlled, as shown in Fig. 5(b). For the gas transport model, it is assumed that coal sample is initially saturated with gas with 0.2 MPa pressure and gas flow only happens in coal matrix (solid part Fig. 5(b)). A constant injection pressure is specified at the boundaries of fracture, but its value varies depending on the requirements of the modelling design. Number of elements is 15,468 and only triangular elements are used. To increase the accuracy of the results around the fracture, mesh density increases from the outer boundary to the fracture boundary. Input parameters for this simulation are listed in Table 1.

3.2. Performance for a homogeneous coal

For this case, coal matrix is assumed to be homogeneous, where Young's modulus and Poisson's ratio are constants and the Langmuir strain constant is same throughout the whole domain. The simulation scenarios are listed in Table 2.

Typical evolution of coal permeability is shown in Fig. 6. As can be seen from it, coal permeability experiences a rapid reduction at the early stage. When the modelled time is about 2000 s, a switch in behaviour from permeability reduction to recovery is observed, after which coal permeability recovers until it reaches the final equilibrium permeability. The final equilibrium permeability is higher than the original value, which is inconsistent with laboratorial observations (Cui et al., 2007; Day et al., 2008; Harpalani and Schraufnagel, 1990; Karacan, 2007; Kiyama et al., 2011; Levine, 1996; Mazumder and Wolf, 2008; Robertson, 2005; Seidle and Huitt, 1995; Wang et al., 2010, 2011). Permeability increase

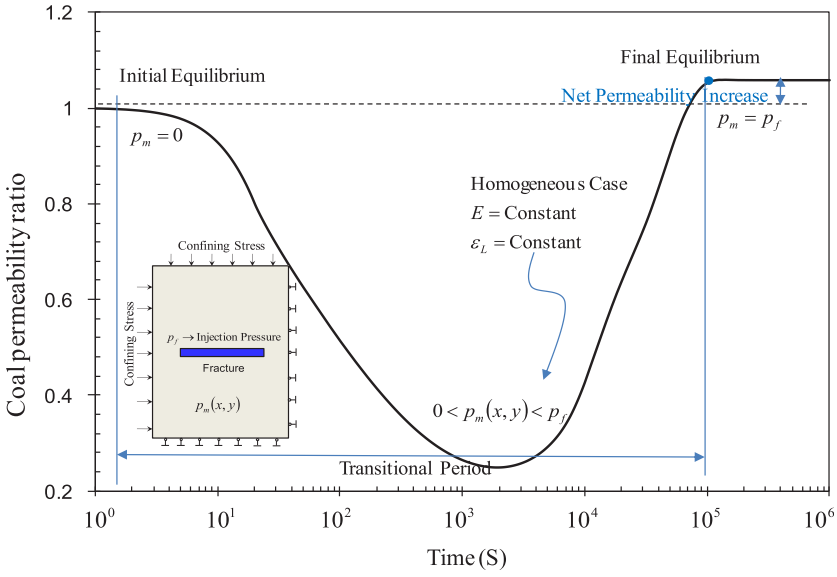

Fig. 6. Numerical result of permeability evolution for the homogeneous coal.

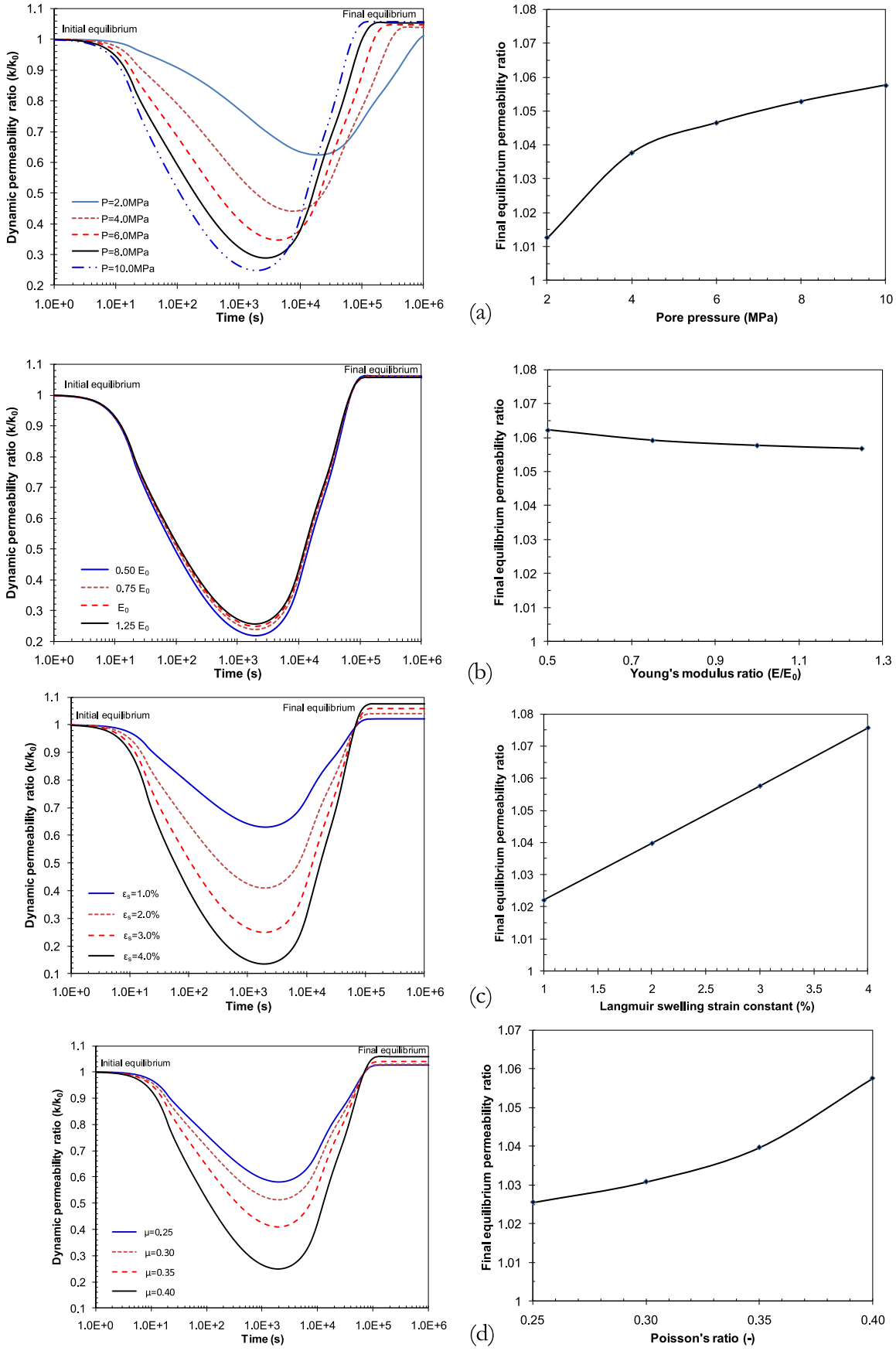

Fig. 7. Variation of both dynamic permeability and equilibrium permeability for a homogeneous coal under the unconstrained swelling condition. (a) Influence of pore pressures; (b) influence of modulus magnitudes; (c) influence of Langmuir strain constants; (d) influence of Poisson's ratios.

with gas injection is obtained for all homogeneous cases as shown in Fig. 7. Final equilibrium permeability increases with increasing fluid pressure, Poisson's ratio and volume swelling strain capacity, but decreases with rising Young's Modulus. The results illustrate that the parameter values only affect the transient variation feature of permeability and the final absolute permeability value, but they have no impact on permeability change trend. In other words, permeability does not decrease no matter what coal physical property values are as long as with homogeneous assumption.

The conceptual understanding on the modelling processes is illustrated in Fig. 8. Prior to the CO_2 injection, the gas pressure in the fracture is equal to that in the matrix. This state is defined as the initial equilibrium state, $p_m = p_f = p_0$, and coal permeability at this state is defined as the initial equilibrium permeability, as illustrated in Fig. 8(a). When CO_2 is injected, the gas occupies the fracture and the gas pressure in the fracture reaches the injection pressure almost instantly. At this stage, the maximum imbalance between fracture pressure and matrix pressure is achieved. But the pressure imbalance diminishes gradually as the gas transports into coal matrix, consequently causes coal matrix to swell. Initially, due to the matrix–fracture interaction, matrix swelling is confined in the vicinity of the fracture voids, so the localized swelling moves towards fracture voids and closes the fracture aperture, and in turn reduces the fracture permeability, as shown in Fig. 8(b). As CO_2 flow progresses, the swelling zone extends further into coal matrix, and the influence of matrix swelling on the fracture aperture weakens. As a result of the widening of the swelling zone, the fracture aperture opening starts to recovers, so is the permeability. When the imbalance between fracture pressure and matrix pressure diminishes completely, the final equilibrium state is achieved, as shown in Fig. 8(c). At this state, the fracture pressure is equal to the matrix pressure, i.e. $p_m = p_f = p_{in}$, where p_{in} is the injection pressure. Coal permeability at this state is defined as the final equilibrium permeability. As coal fracture aperture increases compared with the original value, so the fracture permeability enhances after the swelling. This enhancement includes two factors: the reduction of effective stress due to pore pressure increase, and the sorption-induced fracture aperture increase.

Based on the above analysis, the final equilibrium permeability is always higher than the initial equilibrium permeability if a uniform swelling state is achieved within a coal sample. However, laboratorial measurements show that coal equilibrium permeability is generally much lower than the initial equilibrium permeability in low pore pressure range, may recover but rarely exceeds the initial equilibrium permeability even at high pore pressures. This distinct discrepancy points to a conclusion that a uniform matrix swelling state is rarely achieved in real coal sample tests. Therefore, a difference between the ultimate permeability for an ideal homogeneous coal and that for a real heterogeneous coal is expected.

3.3. Performance for a heterogeneous coal

As summarized in the introduction part, adsorption and swelling processes have been shown to be heterogeneous in coal (Day et al., 2008; Karacan and Okandan, 2001; Karacan, 2003, 2007), thus characteristics for the heterogeneity may include:

(1) Initial distributions of key parameters, including coal Young's modulus (E), permeability (k_0), porosity (ϕ_0), Langmuir strain constant (ε_L), and Langmuir pressure constant (p_L). If any or combination of them varies spatially, coal is considered as initially heterogeneous.
(2) Swelling/shrinkage dependencies of these key parameters, including coal Young's modulus (E), Langmuir strain constant

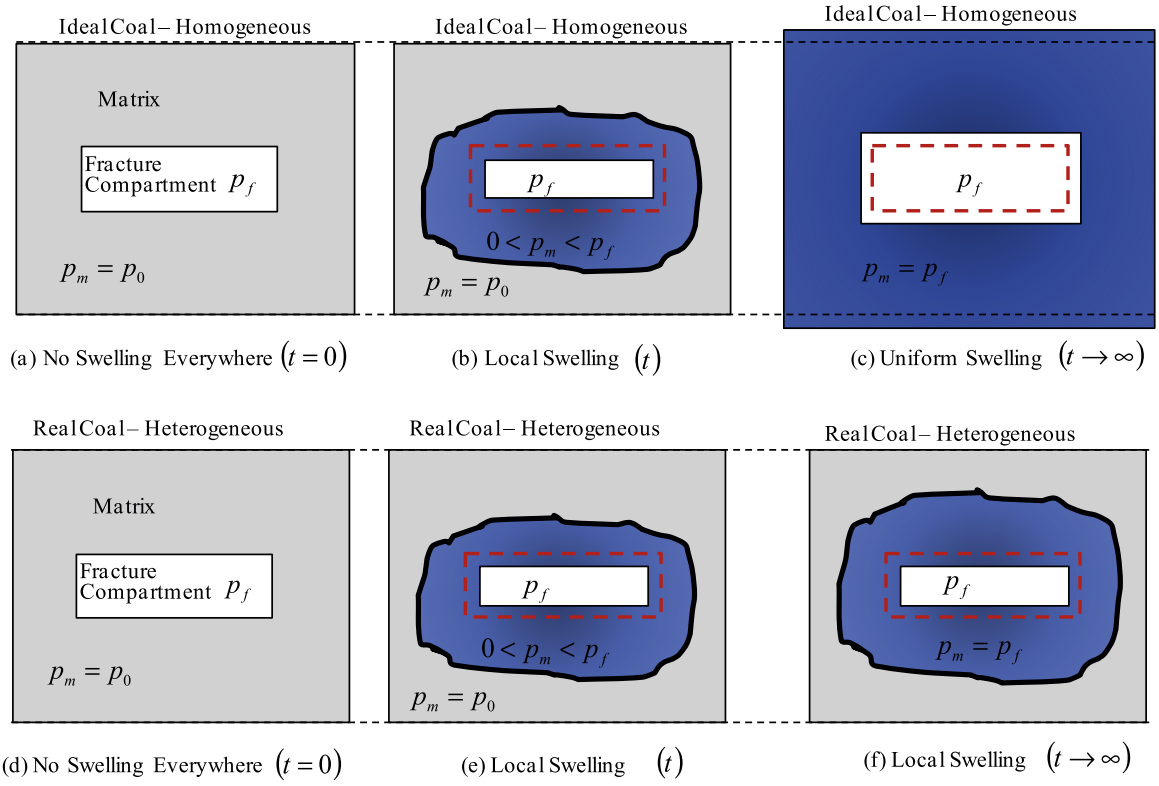

Fig. 8. Illustration of the difference of swelling behaviours between the homogeneous coal and the heterogeneous coal. The red dotted line represents the original location of fracture, and blue colour zone represents the gas diffusion zone. (For interpretation of the references to colour in this figure legend, the reader is referred to the web version of this article.)

(ε_L), and Langmuir pressure constant (p_L). If any or combination of them varies spatially due to gas sorption, coal is considered as swelling heterogeneous.

(3) The ultimate distribution of pore pressure (p) is controlled by boundary conditions. If this distribution is not uniform within coal matrix, a uniform swelling within the matrix is not achievable.

How to represent these heterogeneities more accurately is the key to reduce the difference between the modelled coal permeability and the measured one. In the following section we represent the heterogeneity through spatial distributions of two key parameters – Young's modulus and Langmuir strain constant.

3.3.1. Modelling scenarios for a heterogeneous matrix

We generalize changes in permeability that accompanies gas adsorption under conditions of constant applied stress and for increments of applied gas pressure for fractures. Specifically we explore the relations between coal dynamic (or transient) permeability and equilibrium permeability, and how these relations are controlled both by the distributed coal Young's modulus and Langmuir strain constant, and by the fluid injection pressure. The scenarios simulated in the model are listed in Table 3.

3.3.2. Impacts of heterogeneous Young's modulus

The numerical results are summarized and divided into three groups. This division is based on the reasons for heterogeneity.

Cases 1–3 are for the heterogeneous coal represented by the spatial distribution of coal Young's modulus. In all three cases, coal Young's modulus is considered to decrease linearly from outer boundaries to the inner fracture walls, and its values at the outer boundary and fracture wall are E_0 and αE_0, respectively. α here is defined as coal Young's modulus softening coefficient. Langmuir strain constant is assumed as constant throughout the whole simulated domain.

As shown in Fig. 9, the dynamic permeability evolves from the initial rapid reduction, to recovery, and to a net reduction. The reason for this net reduction is that as the localization extends to the outside boundary, as shown in Fig. 8(e), coal permeability recovers, but the even distribution of effective stress induced strain is not achieved at the equilibrium state because the coal Young's modulus is spatially related. As coal matrix is softer around the fracture walls than outside shell, more strain is expected near fracture walls. Larger deformation is expected to move toward fracture void during the constraint of surround coal media, and then is transferred to the reduction in fracture apertures, as illustrated in Fig. 8(f). Because the uniform deformation can be not reached for this case, the final equilibrium permeability is not as large as that for homogeneous case. However, whether the final permeability is higher than original value or not depends on the extent of heterogeneity, which is reflected by the value of α here. In general, more permeability reduction is expected when α is smaller. Based on the parameters used for this model, the results show that coal equilibrium permeability decreases with increasing gas pore pressure and the Langmuir strain constants, as shown in

Table 3
Simulation scenarios for heterogeneous case.

Simulation scenario	Fracture pressure p_f (MPa)	Young's modulus × E_0	Langmuir strain constant ε_L (%)	Modelling result
Case 1	2.0, 4.0, 6.0, 8.0, 10	Matrix E_0 / Fracture Wall αE_0	3.0	Fig. 9(a)
Case 2	10.0	Matrix E / Fracture Wall αE	3.0	Fig. 9(b)
		0.5, 0.75, 1.0, 1.25		
Case 3	10.0	Matrix E_0 / Fracture Wall αE_0	1.0, 2.0, 3.0, 4.0	Fig. 9(c)
Case 4	2.0, 4.0, 6.0, 8.0, 10	1.0	Matrix $\beta\varepsilon_L$ / Fracture Wall ε_L	Fig. 10(a)
Case 5	10.0	0.5, 0.75, 1.0, 1.25		Fig. 10(b)
Case 6	10.0	1.0	Matrix $\beta\varepsilon_L$ / Fracture Wall ε_L	Fig. 10(c)
			1.0, 2.0, 3.0, 4.0	
Case 7	2.0, 4.0, 6.0, 8.0, 10	Matrix E_0 / Fracture Wall αE_0	Matrix $\beta\varepsilon_L$ / Fracture Wall ε_L	Fig. 11(a)
Case 8	10.0	Matrix E / Fracture Wall αE	Matrix $\beta\varepsilon_L$ / Fracture Wall ε_L	Fig. 11(b)
		0.5, 0.75, 1.0, 1.25		
Case 9	10.0	Matrix E_0 / Fracture Wall αE_0	Matrix $\beta\varepsilon_L$ / Fracture Wall ε_L	Fig. 11(c)
			1.0, 2.0, 3.0, 4.0	

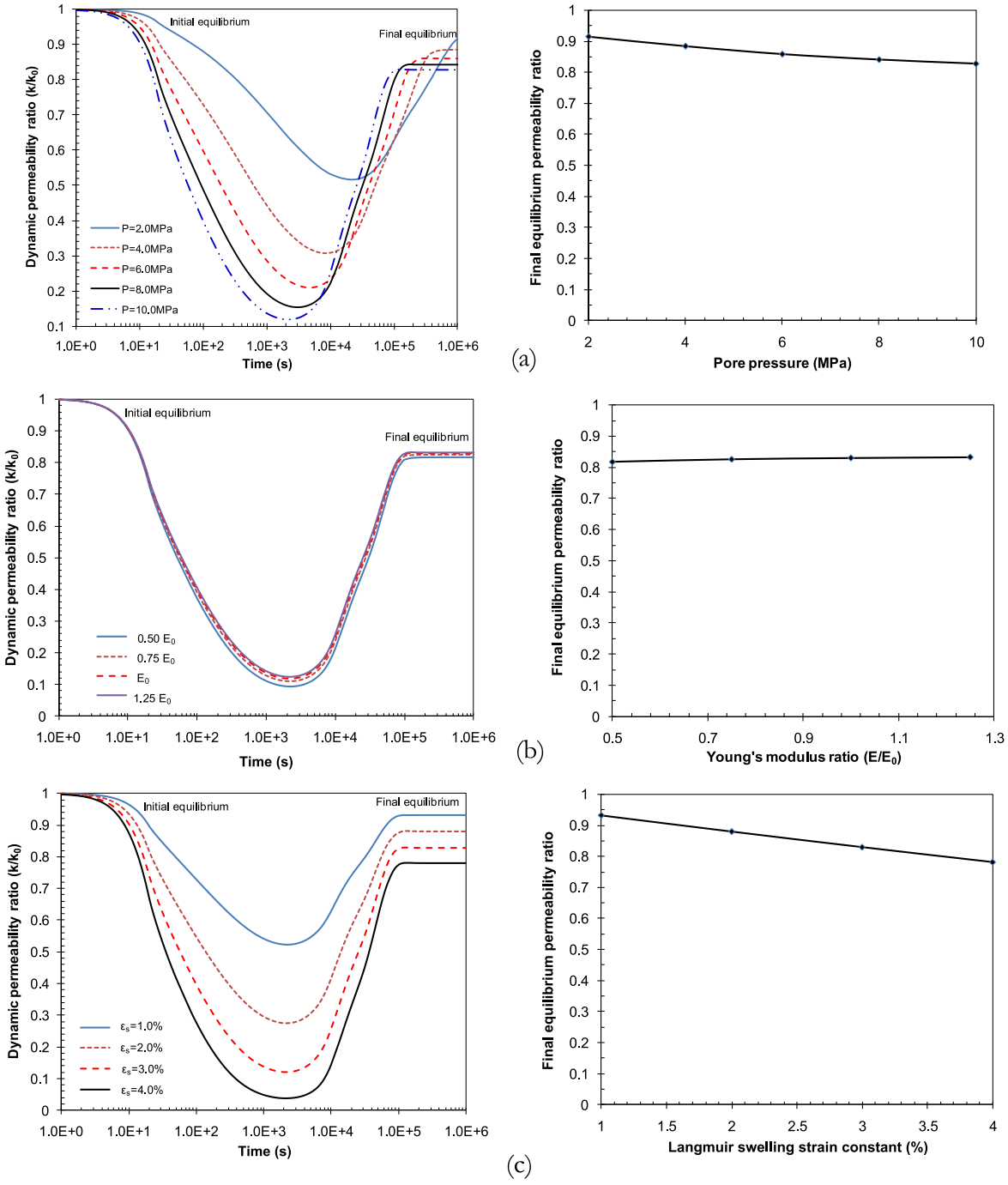

Fig. 9. Variation of both dynamic permeability and final equilibrium permeability for a heterogeneous coal represented by the spatial distribution of coal Young's modulus under the unconstrained swelling condition. (a) Influence of pore pressures; (b) influence of modulus ratios; (c) influence Langmuir strain constants.

Figures 9(a) and (c), and increases with increasing coal Young's modulus changes, as shown in Fig. 9(b).

3.3.3. *Impacts of heterogeneous Langmuir strain constant*

Cases 4–6 are for the heterogeneous coal represented by the spatial distribution of Langmuir strain constant. This constant is considered to decrease linearly from the inner fracture walls to outer boundaries, and its values at the outer boundary and fracture wall are $\beta\varepsilon_L$ and ε_L respectively. β is the newly introduced swelling strain constant reduction factor, and coal Young's modulus is assumed as constant for this scenario. Modelling results are shown in Fig. 10(a)–(c). Similar to the results of cases 1–3, the dynamic permeability of cases 4–6 also evolves from the initial rapid reduction, to recovery, and to a net reduction, but a uniform swelling within coal matrix is not achieved. When coal matrix swelling is localized near the fracture compartment, the swelling of a soft medium is constrained within a rigid outer shell. In this situation, coal sample can be considered as constrained from all directions, and coal matrix swelling is directly transferred to the closure of fracture apertures. This assumption also explains why coal equilibrium permeability decreases at the equilibrium state of gas transport. The results also apply to the scenarios where the equilibrium state (pore pressure is same throughout the whole domain) is not achievable.

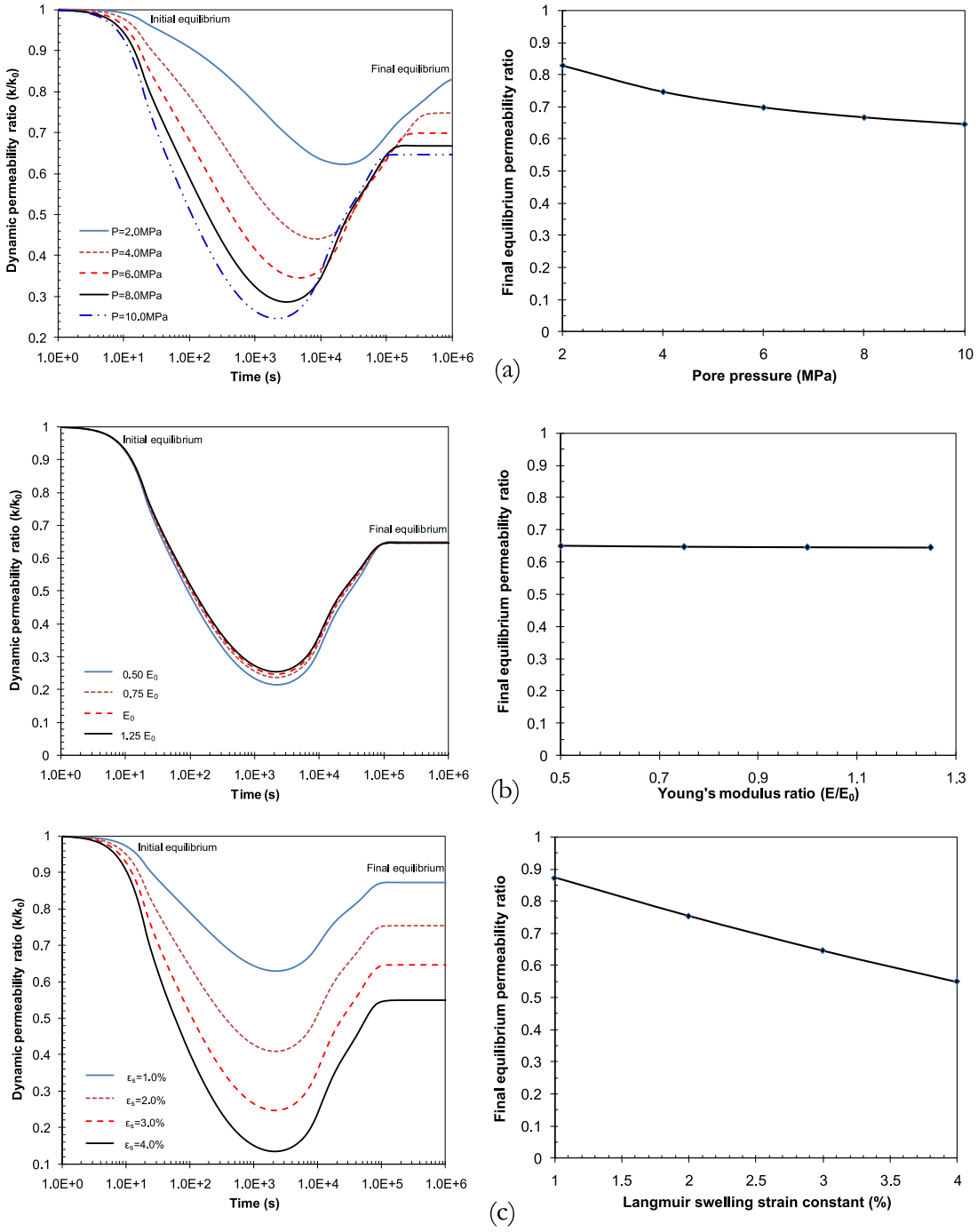

Fig. 10. Variation of both dynamic permeability and final equilibrium permeability for a heterogeneous coal represented by the spatial distribution of Langmuir strain constant under the unconstrained swelling condition. (a) Influence of pore pressures; (b) influence of modulus ratios; (c) influence of Langmuir strain constants.

3.3.4. Combined impact of heterogeneous Langmuir strain and Young's modulus

Cases 7–9 are for the heterogeneous coal represented by the spatial distributions of both coal Young's modulus and Langmuir strain constant. For this scenario, coal Young's modulus is considered to decrease linearly from outer boundaries to the inner fracture walls, and its values at the outer boundary and fracture wall are E_0 and αE_0, respectively. Langmuir strain constant is considered to decrease linearly from the inner fracture walls to outer boundaries, and its values at the outer boundary and fracture wall are $\beta\varepsilon_L$ and ε_L, respectively. In all three cases, the dynamic permeability evolves from the initial rapid reduction, to recovery, and to a net reduction, but more permeability reduction is observed, as shown in Fig. 11(a)–(c). For instance, the maximum equilibrium permeability reduction is around 25% for cases 1–3, permeability decreases by 50% for cases 4–6, and it further decrease by as much as 72% for cases 7–9.

4. Verification with experimental data

In this section, two sets of experimental data measured under stress controlled conditions are used to verify our assumptions. The

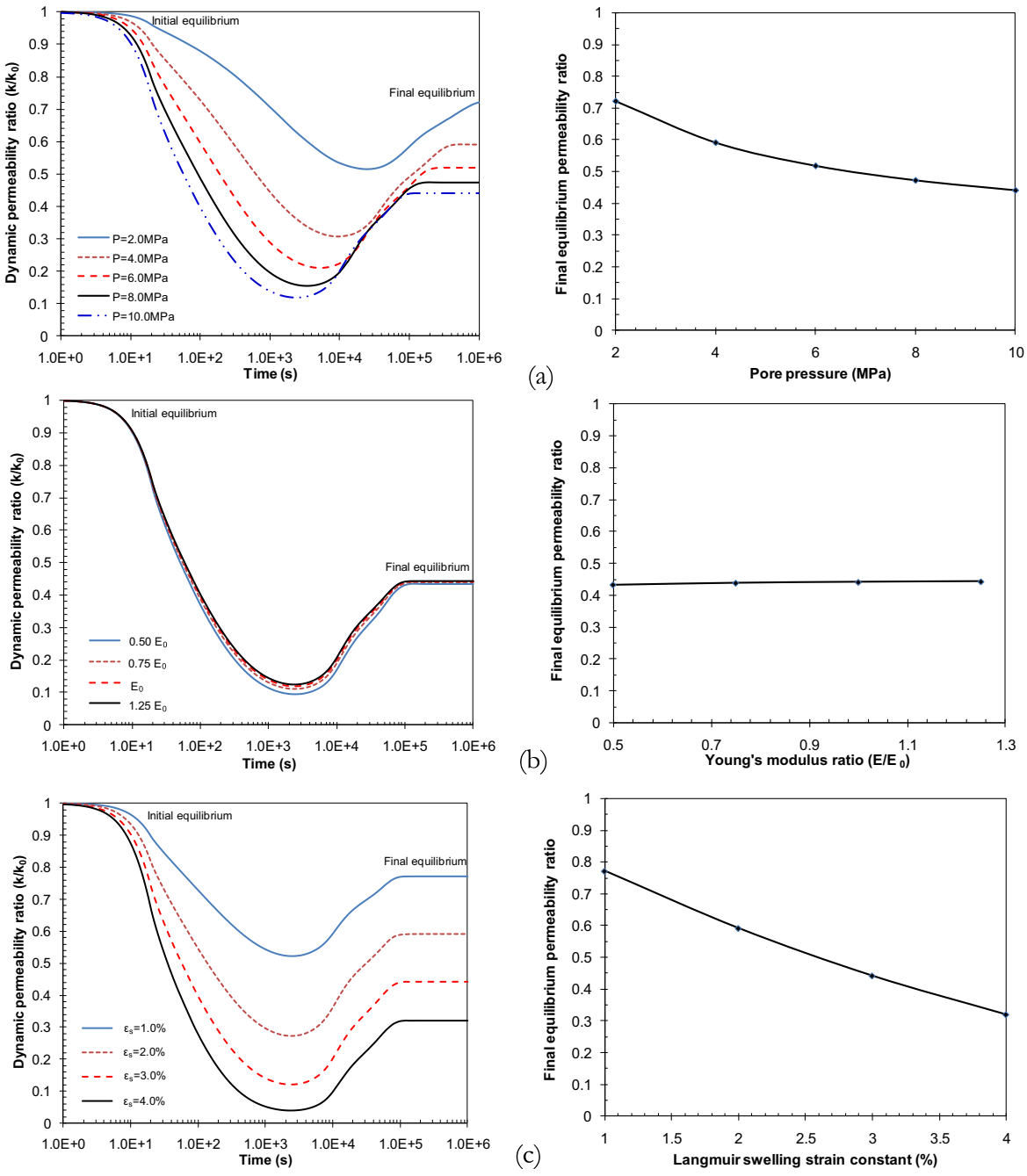

Fig. 11. Variations of both dynamic permeability and final equilibrium permeability for a heterogeneous coal represented by the spatial distributions of both coal Young's modulus and Langmuir strain constant under the unconstrained swelling condition. (a) Influence of pore pressures; (b) influence of initial modulus; (c) influence of initial Langmuir strain constants.

first experimental data comparison is based on the work of Harpalani and Chen (1997), where the confining stress was kept constant throughout the whole measurements. CH_4 was used and permeability variation with decreasing gas pressures (from 6.2 MPa to 0.62 MPa) was measured. The data for the second comparison is from the work of Lin et al. (2008). Permeability of dry composite coal core to CH_4 was measured with constant effective stress of 300 psi (2.07 MPa).

Both homogeneous and heterogeneous models are used to match two sets of data. As only very limited parameters are available in both references, only the CH_4 adsorption parameters are original from Lin et al. (2008), other parameters are given based on the information available from different studies and they are assumed to be same in both comparisons. For instance, coal matrix porosity of 5% is used (Pan and Connell, 2007). As this parameter only affects the time takes to reach the equilibrium phase, and has no impact on the final permeability value, so it is believed that the value is appropriate. The selection of Young's modulus and matrix permeability values are based on the studies of Pan et al. (2010a) and Han et al. (2010). Because the original fracture permeability for Lin et al. (2008) is around four times higher than that of Harpalani and Chen (1997), the matrix permeability is also assumed following the similar trend, as shown in Table 4.

Table 4
Parameters used for data match.

Parameter	Harpalani and Chen (1997)	Lin et al. (2008)
Matrix porosity, %	5.0	5.0
Matrix permeability, m^2	5.0×10^{-22}	2.0×10^{-21}
Viscosity, Pa*s	1.228×10^{-5}	1.228×10^{-5}
Matrix Young's modulus, GPa	1.45	1.45
Poisson's ratio	0.4	0.4
Maximum volumetric swelling strain	0.005	0.0087
Langmuir sorption constant, m^3/kg	0.0132	0.0189
Langmuir pressure constant, MPa	3.96	1.97
Coal density, kg/m^3	1500	1500
Young's modulus softening coefficient, α	0.79	0.555
Swelling strain reduction ratio, β	0.21	0.445

In the homogeneous model, constant Young's modulus and swelling strain capacity are used. In the heterogeneous model, the same assumptions for both coal Young's modulus and Langmuir strain constant is adapted as illustrated earlier. The Young's modulus softening coefficient, α, and swelling strain reduction ratio, β, are considered as variables, and their summation is kept to be 1.0. This is to reflect the interconnection of coal property and swelling strain capacity. The other parameter values used in data matching are listed in Table 4.

Gas flow in the coal matrix only is simulated, and dynamic coal fracture permeability is calculated based on the fracture opening change. For the comparisons, only the final permeability values are used. Take Fig. 12 for instance, the permeability ratio for the point with the pore pressure of 1.66 MPa is the permeability when gas flow reaches equilibrium. Numerical results as plotted in Figs. 12 and 13 show that coal permeability value with homogeneous assumption increases with increasing gas pressure, which is opposite to experimental data, so it is incapable of matching experimental data, but the heterogeneous model with the spatial distributions of both coal Young's modulus and Langmuir strain is capable of replicating the phenomena, and matches experimental data reasonably well. Therefore, it proves that coal heterogeneity assumption adopted in this study is reasonable.

5. Conclusions

The performance of current coal permeability models was evaluated against analytical solutions for the two extreme cases of either unconstrained swelling or constrained swelling. Constrained model predictions are apparently consistent with both typical laboratory measurements and in-situ observations. However, this apparent consistency is due to the mismatch between model boundary condition assumptions (constrained) and experiment boundary condition (unconstrained). This conclusion demonstrates that current permeability models are incapable of explaining net reductions in coal permeability where swelling is unconstrained.

With the inclusion of the heterogeneous distributions of coal physical and swelling properties, a fully coupled approach was applied to investigate coal permeability response under the unconstrained swelling conditions. Based on our model results, the following major conclusions were drawn:

- Both homogeneous and heterogeneous models experience the swelling transition from local swelling to macro swelling. At the initial stage of gas injection, matrix swelling is localized within the vicinity of the fracture compartment. As the injection continues, the swelling zone is widening further into the matrix and becomes macro-swelling.
- Coal permeability experiences a rapid reduction at the early stage, a switch in behaviour from permeability reduction to recovery is observed, and coal permeability finally recovers until it reaches the final equilibrium permeability. For the homogeneous case, the final equilibrium permeability is always higher than the initial value, but the opposite is obtained for the heterogeneous case.
- With the heterogeneous distributions of coal physical and swelling properties, this numerical model matches with the experimental data reasonably well, which demonstrates that heterogeneity assumption of coal properties is reasonable in explaining the permeability reduction under unconstrained conditions.

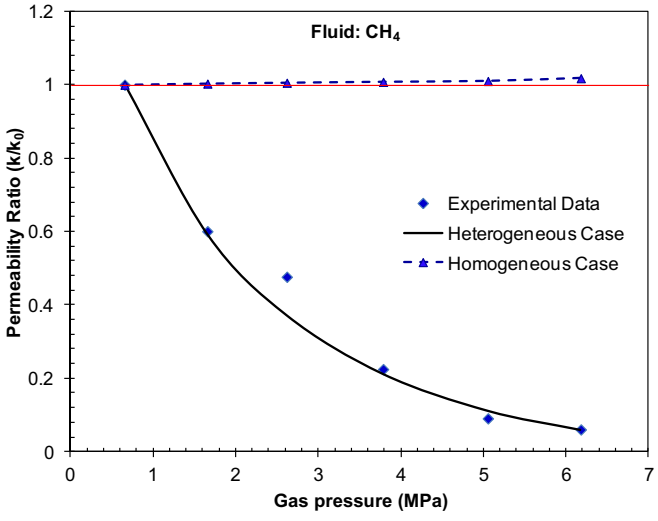

Fig. 12. Measured variation in permeability with decreasing gas pressure (Harpalani and Chen, 1997).

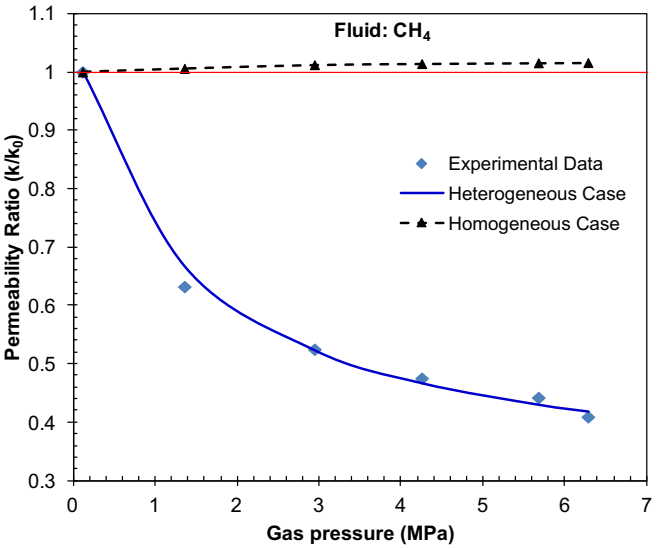

Fig. 13. Permeability of dry composite coal core to CH_4. Effective stress equals to 300 psi (Lin et al., 2008).

Acknowledgements

This work was partially supported by new staff start-up grant from the University of Queensland, UWA-UQ BRCA grant, and Chinese National Science Foundation (51104147). These sources of support are gratefully acknowledged.

References

Ates, Y., Barron, K., 1988. The effect of gas sorption on the strength of coal. Min. Sci. Technol. 6, 291–300.

Chen, Z., Liu, J., Elsworth, D., Connell, L., Pan, Z., 2009. Investigation of CO_2 Injection Induced Coal–Gas Interactions, 43rd U.S. Rock Mechanics Symposium & 4th U.S. – Canada Rock Mechanics Symposium. American Rock Mechanics Association, Asheville, North Carolina.

Chen, Z., Liu, J., Elsworth, D., Connell, L.D., Pan, Z., 2010. Impact of CO_2 injection and differential deformation on CO_2 injectivity under in-situ stress conditions. Int. J. Coal Geol. 81, 97–108.

Chen, Z., Pan, Z., Liu, J., Connell, L.D., Elsworth, D., 2011. Effect of the effective stress coefficient and sorption-induced strain on the evolution of coal permeability: experimental observations. Int. J. Greenh. Gas Control 5, 1284–1293.

Cherian, B.V., Claugus, A.O., Dilli, M., Mata, D., Sitchler, J., Alatrach, S., Neumiller, J.L., Panjaitan, M.L., 2010. An integrated single-well approach to evaluating completion effectiveness and reservoir properties in the Wind Dancer field. In: Tight Gas Completions Conference. Society of Petroleum Engineers, San Antonio, Texas, USA.

Chilingar, G.V., 1964. Relationship between porosity, permeability, and grain-size distribution of sands and sandstones. In: Straaten, L.M.J.U.v. (Ed.), Developments in Sedimentology. Elsevier, pp. 71–75.

Clarkson, C.R., Jordan, C.L., et al., 2008. Production data analysis of coalbed-methane wells. SPE Reserv. Eval. Eng. 11 (2), 311–325.

Clarkson, C.R., Pan, Z., et al., 2010. Predicting sorption-induced strain and permeability increase with depletion for coalbed-methane reservoirs. SPE J. 15 (1), 152–159.

Connell, L.D., 2009. Coupled flow and geomechanical processes during gas production from coal seams. Int. J. Coal Geol. 79, 18–28.

Connell, L.D., Detournay, C., 2009. Coupled flow and geomechanical processes during enhanced coal seam methane recovery through CO_2 sequestration. Int. J. Coal Geol. 77, 222–233.

Connell, L.D., Lu, M., Pan, Z., 2010. An analytical coal permeability model for tri-axial strain and stress conditions. Int. J. Coal Geol. 84, 103–114.

Cui, X., Bustin, R.M., 2005. Volumetric strain associated with methane desorption and its impact on coalbed gas production from deep coal seams. AAPG Bull. 89, 1181–1202.

Cui, X., Bustin, R.M., Chikatamarla, L., 2007. Adsorption-induced coal swelling and stress: implications for methane production and acid gas sequestration into coal seams. J. Geophys. Res. 112, B10202.

Day, S., Fry, R., Sakurovs, R., 2008. Swelling of Australian coals in supercritical CO_2. Int. J. Coal Geol. 74, 41–52.

Douglas, B., 1984. Microscopic in-situ studies of the solvent-induced swelling of thin sections of coal. Fuel 63, 1324–1328.

Durucan, S., Edwards, J.S., 1986. The effects of stress and fracturing on permeability of coal. Min. Sci. Technol. 3, 205–216.

French, D.C., Dieckman, S.L., Botto, R.E., 1993. Three-dimensional NMR microscopic imaging of coal swelling in pyridine. Energy Fuels 7, 90–96.

Gathitu, B.B., Chen, W.-Y., McClure, M., 2009. Effects of coal interaction with supercritical CO_2: physical structure. Ind. Eng. Chem. Res. 48, 5024–5034.

Gibbins, J.R., Beeley, T.J., Crelling, J.C., Scott, A.C., Skorupska, N.M., Williamson, J., 1999. Observations of heterogeneity in large pulverized coal particles. Energy Fuels 13, 592–601.

Goodman, A.L., Favors, R.N., Hill, M.M., Larsen, J.W., 2005. Structure changes in Pittsburgh no. 8 coal caused by sorption of CO_2 gas. Energy Fuels 19, 1759–1760.

Gu, F., Chalaturnyk, J.J., 2005. Analysis of Coalbed Methane Production by Reservoir and Geomechanical Coupling Simulation.

Gu, F., Chalaturnyk, R.J., 2006. Numerical Simulation of Stress and Strain due to Gas Sorption/desorption and Their Effects on In Situ Permeability of Coalbeds.

Han, F., Busch, A., van Wageningen, N., Yang, J., Liu, Z., Krooss, B.M., 2010. Experimental study of gas and water transport processes in the inter-cleat (matrix) system of coal: anthracite from Qinshui Basin, China. Int. J. Coal Geol. 81, 128–138.

Harpalani, S., Chen, G., 1997. Influence of gas production induced volumetric strain on permeability of coal. Geotech. Geol. Eng. 15, 303–325.

Harpalani, S., Schraufnagel, R.A., 1990. Shrinkage of coal matrix with release of gas and its impact on permeability of coal. Fuel 69, 551–556.

Hsieh, S.T., Duda, J.L., 1987. Probing coal structure with organic vapour sorption. Fuel 66, 170–178.

Izadi, G., Wang, S., Elsworth, D., Liu, J., Wu, Y., Pone, D., 2011. Permeability evolution of fluid-infiltrated coal containing discrete fractures. Int. J. Coal Geol. 85, 202–211.

John, W.,L., 2004. The effects of dissolved CO_2 on coal structure and properties. Int. J. Coal Geol. 57, 63–70.

Karacan, C.Ö., 2003. Heterogeneous sorption and swelling in a confined and stressed coal during CO_2 injection. Energy Fuels 17, 1595–1608.

Karacan, C.Ö., 2007. Swelling-induced volumetric strains internal to a stressed coal associated with CO_2 sorption. Int. J. Coal Geol. 72, 209–220.

Karacan, C.O., Okandan, E., 2001. Adsorption and gas transport in coal microstructure: investigation and evaluation by quantitative X-ray CT imaging. Fuel 80, 509–520.

Kiyama, T., Nishimoto, S., Fujioka, M., Xue, Z., Ishijima, Y., Pan, Z., Connell, L.D., 2011. Coal swelling strain and permeability change with injecting liquid/supercritical CO_2 and N_2 at stress-constrained conditions. Int. J. Coal Geol. 85, 564.

Larsen, J.W., 2004. The effects of dissolved CO_2 on coal structure and properties. Int. J. Coal Geol. 57, 63–70.

Levine, J.R., 1996. Model study of the influence of matrix shrinkage on absolute permeability of coal bed reservoirs. In: Gayer, R., Harris, I. (Eds.), Coalbed Methane and Coal Geology, Geological Society Special Publication No 109. London, pp. 197–212.

Lin, W., Tang, G.-Q., Kovscek, A.R., 2008. Sorption-induced permeability change of coal during gas-injection processes. SPE Reserv. Eval. Eng. 11 (4), 792–802. SPE-109855-PA.

Liu, C.J., Wang, G.X., Sang, S.X., Rudolph, V., 2010. Changes in pore structure of anthracite coal associated with CO_2 sequestration process. Fuel 89, 2665–2672.

Liu, H.-H., Rutqvist, J., 2010. A new coal-permeability model: internal swelling stress and fracture–matrix interaction. Transp. Porous Media 82, 157–171.

Liu, J., Chen, Z., Elsworth, D., Miao, X., Mao, X., 2010a. Evaluation of stress-controlled coal swelling processes. Int. J. Coal Geol. 83, 44455.

Liu, J., Chen, Z., Elsworth, D., Miao, X., Mao, X., 2010b. Linking gas-sorption induced changes in coal permeability to directional strains through a modulus reduction ratio. Int. J. Coal Geol. 83, 21–30.

Liu, J., Chen, Z., Elsworth, D., Qu, H., Chen, D., 2011a. Interactions of multiple processes during CBM extraction: a critical review. Int. J. Coal Geol. 87, 175–189.

Liu, J., Wang, J., Chen, Z., Wang, S., Elsworth, D., Jiang, Y., 2011b. Impact of transition from local swelling to macro swelling on the evolution of coal permeability. Int. J. Coal Geol. 88, 31–40.

Maggs, F.A.P., 1946. The adsorption-swelling of several carbonaceous solids. Trans. Faraday Soc. 42, B284–B288.

Manovic, V., Loncarevic, D., Tokalic, R., 2009. Particle-to-particle heterogeneous nature of coals—a case of large coal particles. Energy Sources A Recovery Util. Environ. Eff. 31, 427–437.

Mazumder, S., Wolf, K.H., 2008. Differential swelling and permeability change of coal in response to CO_2 injection for ECBM. Int. J. Coal Geol. 74, 123–138.

Mirzaeian, M., Hall, P.J., 2006. The interactions of coal with CO_2 and its effects on coal structure. Energy Fuels 20, 2022–2027.

Mirzaeian, M., Hall, P.J., 2008. Thermodynamical studies of irreversible sorption of CO_2 by Wyodak coal. J. Chem. Chem. Eng. 27, 59–68.

Palmer, I., Mansoori, J., 1998. How permeability depends on stress and pore pressure in coalbeds: a new model. SPE Reserv. Eval. Eng. 1 (6), 539–544.

Pan, Z., Connell, L.D., 2007. A theoretical model for gas adsorption-induced coal swelling. Int. J. Coal Geol. 69 (4), 243–252.

Pan, Z., Connell, L.D., Camilleri, M., 2010a. Laboratory characterisation of coal reservoir permeability for primary and enhanced coalbed methane recovery. Int. J. Coal Geol. 82, 252–261.

Pan, Z., Connell, L.D., Camilleri, M., Connelly, L., 2010b. Effects of matrix moisture on gas diffusion and flow in coal. Fuel 89, 3207–3217.

Pekot, L.J., Reeves, S.R., 2002. Modeling the Effects of Matrix Shrinkage and Differential Swelling on Coalbed Methane Recovery and Carbon Sequestration. U.S. Department of Energy. DE-FC200NT40924.

Pini, R., Ottiger, S., Burlini, L., Storti, G., Mazzotti, M., 2009. Role of adsorption and swelling on the dynamics of gas injection in coal. J. Geophys. Res. 114, B04203.

Pone, J.D.N., Halleck, P.M., Mathews, J.P., 2010. 3D characterization of coal strains induced by compression, carbon dioxide sorption, and desorption at in-situ stress conditions. Int. J. Coal Geol. 82, 262–268.

Ranjith, P.G., Jasinge, D., Choi, S.K., Mehic, M., Shannon, B., 2010. The effect of CO_2 saturation on mechanical properties of Australian black coal using acoustic emission. Fuel 89, 2110–2117.

Robertson, E.P., 2005. Modeling permeability in coal using sorption-induced strain data. In: SPE Annual Technical Conference and Exhibition. Society of Petroleum Engineers, Dallas, Texas.

Seidle, J.R., Huitt, L.G., 1995. Experimental Measurement of Coal Matrix Shrinkage Due to Gas Desorption and Implications for Cleat Permeability Increases. International Meeting on Petroleum Engineering. Society of Petroleum Engineers, Inc, Beijing, China.

Shi, J.Q., Durucan, S., 2004. Drawdown induced changes in permeability of coalbeds: a new interpretation of the reservoir response to primary recovery. Transp. Porous Media 56, 1–16.

Siriwardane, H., Haljasmaa, I., McLendon, R., Irdi, G., Soong, Y., Bromhal, G., 2009. Influence of carbon dioxide on coal permeability determined by pressure transient methods. Int. J. Coal Geol. 77, 109–118.

Somerton, W.H., Söylemezoglu, I.M., Dudley, R.C., 1975. Effect of stress on permeability of coal. Int. J. Rock Mech. Min. Sci. Geomech. Abstr. 12, 129–145.

Sparks, D.P., McLendon, T.H., Saulsberry, J.L., Lambert, S.W., 1995. The effects of stress on coalbed reservoir performance, Black Warrior Basin, U.S.A. In: SPE Annual Technical Conference and Exhibition. Society of Petroleum Engineers, Inc, Dallas, Texas. Copyright 1995.

Viete, D.R., Ranjith, P.G., 2006. The effect of CO_2 on the geomechanical and permeability behaviour of brown coal: implications for coal seam CO_2 sequestration. Int. J. Coal Geol. 66, 204–216.

Viete, D.R., Ranjith, P.G., 2007. The mechanical behaviour of coal with respect to CO_2 sequestration in deep coal seams. Fuel 86, 2667–2671.

Walsh, J.B., Grosenbaugh, M.A., 1979. A new model for analyzing the effect of fractures on compressibility. J. Geophys. Res. Solid Earth 84, 3532–3536.

Wang, G.X., Wei, X.R., Wang, K., Massarotto, P., Rudolph, V., 2010. Sorption-induced swelling/shrinkage and permeability of coal under stressed adsorption/desorption conditions. Int. J. Coal Geol. 83, 454.

Wang, S., Elsworth, D., Liu, J., 2011. Permeability evolution in fractured coal: the roles of fracture geometry and water-content. Int. J. Coal Geol. 87, 13–25.

White, C.M., Smith, D.H., Jones, K.L., Goodman, A.L., Jikich, S.A., LaCount, R.B., DuBose, S.B., Ozdemir, E., Morsi, B.I., Schroeder, K.T., 2005. Sequestration of carbon dioxide in coal with enhanced coalbed methane recovery: a review. Energy Fuels 19, 659–724.

Yasuhara, H., Elsworth, D., 2008. Compaction of a rock fracture moderated by competing roles of stress corrosion and pressure solution. Pure Appl. Geophys. 165, 1289–1306.

Young, G.B.C., McElhiney, J.E., Paul, G.W., McBane, R.A., 1991. An analysis of Fruitland coalbed methane production, Cedar Hill field, northern San Juan Basin. In: SPE Annual Technical Conference and Exhibition. Society of Petroleum Engineers, Inc, Dallas, Texas. Copyright 1991.

Zhang, H., Liu, J., Elsworth, D., 2008. How sorption-induced matrix deformation affects gas flow in coal seams: a new FE model. Int. J. Rock Mech. Min. Sci. 45, 1221236.